

Article

Spatiotemporal Distribution and Influencing Factors of the Net Primary Productivity in the Datai Mine in Western Beijing

Linda Dai ^{1,*}, Yongliang Zhang ^{1,2}, Rijia Ding ¹ and Yueguan Yan ³ ¹ School of Management, China University of Mining & Technology (Beijing), Beijing 100083, China² State Key Laboratory of Water Resource Protection and Utilization in Coal Mining, Beijing 102209, China³ College of Geoscience and Surveying Engineering, China University of Mining & Technology (Beijing), Beijing 100083, China

* Correspondence: bqt2000503020@student.cumtb.edu.cn

Abstract: In the context of those countries around the world that are actively promoting sustainable development of the environment, China has formulated a new “double carbon” strategic goal to assume corresponding responsibilities. Vegetation carbon sequestration plays a key role in enhancing the carbon sink capacity toward reaching the carbon peak and carbon neutrality. In order to quantitatively study vegetation carbon sequestration, in this article, we used the net primary productivity (NPP) as an indicator to measure it. In this research, the Datai Coal Mine in western Beijing was used as the study area, and the spatiotemporal distribution characteristics and the influencing factors of carbon sequestration through vegetation were analyzed. Based on the meteorological data, remote sensing images, and the land use data of the mining area, the improved Carnegie–Ames–Stanford Approach (CASA) was used to calculate the net primary productivity (NPP) of vegetation in the Datai mining area from 2013 to 2021, to analyze its temporal and spatial distribution in relation to meteorological factors. The results showed that in the past 9 years, the NPP in the Datai mining area generally increased from 546 gC/m² to 601 gC/m². The NPP in the Mentougou District generally decreased and had a significant relationship with precipitation, temperature, and solar radiation. The Mentougou District’s NPP change had a significant positive correlation with the precipitation change ($R^2 = 0.8$). The Mentougou District’s NPP change had no significant relationship with temperature ($R^2 = 0.98$) and solar radiation fluctuations ($R^2 = 0.75$). In conclusion, the vegetation NPP in the Datai Mine regularly changed throughout the year, and its annual vegetation NPP was about twice that of the Mentougou District, which probably due to the low-intensity mining of the Datai Mine. Thus, there is no significant impact on the vegetation carbon in this area.

Keywords: net primary productivity; meteorological drivers; spatiotemporal distribution

Citation: Dai, L.; Zhang, Y.; Ding, R.; Yan, Y. Spatiotemporal Distribution and Influencing Factors of the Net Primary Productivity in the Datai Mine in Western Beijing. *Sustainability* **2022**, *14*, 15567. <https://doi.org/10.3390/su142315567>

Academic Editor: Antonio Miguel Martínez-Graña

Received: 23 October 2022

Accepted: 19 November 2022

Published: 23 November 2022

Publisher’s Note: MDPI stays neutral with regard to jurisdictional claims in published maps and institutional affiliations.



Copyright: © 2022 by the authors. Licensee MDPI, Basel, Switzerland. This article is an open access article distributed under the terms and conditions of the Creative Commons Attribution (CC BY) license (<https://creativecommons.org/licenses/by/4.0/>).

1. Introduction

Achieving the “double carbon” goal of peak carbon dioxide emissions in 2030 and carbon neutrality by 2060 is a major strategic decision made by China for the construction of ecological civilization. This is not only a solemn commitment to all countries in the world but also, domestically, an inherent requirement for sustainable development [1]. The “Carbon Peaking Action Plan before 2030” project has formulated by the State Council in 2021. In order to solve the issues in the ecological restoration projects of abandoned historical mines, the consolidation and improvement of the carbon sink capacity is listed as a critical task, and it is proposed that the restoration and management of degraded land be strengthened. As one of the most critical factors affecting the ecological environment, climate change directly impacts the structure and distribution of vegetation types [2,3]. The estimation of the NPP of vegetation can directly reflect the response of the terrestrial ecosystem to climate change and its multi-scale interaction process [4–6]. Therefore, it is of great significance to study the calculation of vegetation carbon sequestration in coal mining areas and analyze the impact of climate change on vegetation carbon sequestration.

The commonly used carbon sequestration calculation methods are divided into direct observation and model measurement methods. Some authors measured the net photosynthetic rate of plants by using a photosynthesis monitor, calculated the fixed carbon dioxide mass and released oxygen mass of the vegetation leaf area in a single day, and then used a canopy analyzer to measure the vegetation leaf area index [7,8]. Finally, the photosynthetic rate method was used to calculate the carbon sequestration of plants. Although this method can obtain the dynamic changes in vegetation carbon sequestration, it is suitable for measuring vegetation carbon sequestration in urban green areas, parks, and other similar environments. Meanwhile, the measurement takes a long time, and it is difficult to obtain the annual change law of vegetation [9]. Although the carbon density method can measure carbon sequestration over a large scale in areas with a high density of vegetation, it requires the measurement and recording of data such as breast height and diameter for all the trees in a sample plot one by one, which requires a large workload, with specific requirements for the measurement environment, and is unsuitable for areas with small space [10–12].

Thus, since it is difficult to directly and accurately measure the carbon sequestration of vegetation by using ordinary positioning and observation methods, relevant scholars use other indicators to measure the carbon sequestration of vegetation, one of which is the net primary productivity (NPP) of surface vegetation [13]. The NPP refers to the ability of plants to use solar light for photosynthesis to fix and convert inorganic carbon (CO_2) into organic carbon. It is the leading indicator for measuring carbon sinks in terrestrial ecosystems [14,15].

Furthermore, there are four main types of models used to measure the vegetation NPP: climate–productivity relationship models, ecophysiological process models, remote sensing application models, and light utilization efficiency models. Climate–productivity relationship models are established on the basis of the relationship between the net primary productivity of vegetation and the climate in the early stage of research, and based on these models, some papers analyzed the current situation of the vegetation NPP in China and provided targeted suggestions for improving it under different meteorological environments. However, although the parameters of this type of model are easy to obtain, the estimation process is based on point and surface [16]. Therefore, some scholars have established ecophysiological process models, which are based on the vegetation growth process combined with soil factors based on climatic factors [17,18]. The estimation results of this type of model are relatively accurate. Although the impact of climate change on the vegetation NPP can be further stimulated, this model is rather complex in that it is challenging to obtain the parameter data and difficult to convert the scale of the study area. Thus, it is impossible to research the mining area. There are two main methods of combining remote sensing application models. The first is the optimized production efficiency model (PEM), which is simpler than the environmental and physiological process model in measuring the vegetation NPP [19]. However, the leaf area index (LAI), one of the critical parameters of this model, greatly influences the overall measurement of the NPP, so the measurement accuracy of the LAI is exceptionally high. The second method is the FOREST-BGC model, which improves the applicability of the ecophysiological process model [20]. Combined with the LAI obtained with remote sensing, this model can measure the daily average and the annual average vegetation NPP [21]. Although light utilization efficiency models can reflect the changes in vegetation information when calculating the NPP over time, these models are also relatively complex, and human intervention factors during the establishment of their parameters affect the accuracy of vegetation NPP calculations. The most widely used light utilization efficiency model is the CASA model. One investigation found when use traditional CASA models to estimate the vegetation NPP in China, the value of NPP is generally smaller than real NPP value. The reason is the default value of the maximum light energy utilization rate (0.389 g of carbon per joule) in traditional model was not applicable in China [22,23]. In a follow-up study, Zhu (2005) improved the CASA model by adding the vegetation coverage classification data,

simulated the maximum light energy utilization rate of different vegetation types according to the vegetation NPP measurement results, and calculated the NPP in China from 1989 to 1993. In the CASA model, although the vegetation parameters are easy to obtain, and the scale conversion of the research area is convenient, the vegetation NPP cannot be simulated and predicted. Therefore, selecting an appropriate model to estimate the vegetation NPP has essential research significance for the restoration of the ecological environment and the rational development of natural resources [24,25].

Therefore, in this study, we combined the improved CASA model with remote sensing data to analyze the temporal and spatial variations in carbon sequestration under low mining intensity. The relationship between meteorological factors and the NPP at the mining area scale was analyzed. This article aimed to remedy the deficiencies of previous research on the NPP of vegetation in small mining areas. The article also aimed to supplement the study of high-precision spatiotemporal changes in the NPP based on long time series for low mining intensity mining area. This method was applied to study areas with similar mountainous landforms and under the low-intensity mining conditions of small coal mines.

Moreover, the aim of this article was to research the spatiotemporal variation characteristics of the NPP in western Beijing's Datai Mine from 2013 to 2021 in order to understand the impact of meteorological elements and coal mining on the NPP. Based on this goal, we used the improved CASA model to calculate the NPP. The spatial and temporal distributions of the NPP over long-term periods of the entire Mentougou District were analyzed. Based on nonlinear fitting, this article used the functional formula to interpret the relationships between climate and the NPP. Through the functions the most suitable growth conditions of vegetation were found. The results of this article are helpful to provide more positive methods to enhance ecosystems and may be applicable to study areas with similar mountainous landforms and under the low-intensity mining conditions of small coal mines.

2. Material and Method

2.1. Selection of Study Area and Contrast Area

In this paper, the Datai Mine was used as the study area, and by considering the influence of the mining range of the mining area on the surface, the longitude and latitude range of the Datai Mine study area was determined; therefore, the plot of the coal mining area encompassed the inflection point coordinates of 40 minefields in the mining area. In order to compare the carbon sequestration patterns between the mining area and the non-mining area, we selected a contrast area with the same scale, which had also similar ecological factors, such as geological conditions, meteorological environments, and topographic characteristics (Figure 1).

2.2. General Situation of Datai Mine

The Datai Mine is located in western Beijing's mining area in the Mentougou District, Beijing City. The mine was formally established in 1958, with a designed production capacity of 600 kt/a and an actual production capacity of 800 kt/a. It was closed in September 2019. The mine has a mining history of 61 years and is a representative steep seam coal mine in China. The mine strike is 10.8 km long. A contrast chart of the upper and lower wells of the Datai Mine is shown in Figure 2a. Eight coal seams can be mined, the total coal thickness is 12.5 m, and the coal seam inclination is 45~88°. The mining elevation of the coal seam is +400~-500 m. The coal seam of the mine is divided into nine mining levels, and the bottom elevations of each level are, respectively, +288 m, +190 m, +90 m, -10 m, -110 m, -210 m, -310 m, -410 m, and -510 m. The mine adopts vertical shaft and inclined shaft mining mode, and adopts a series of cross-holes pass through coal seam group; the geological section is shown in Figure 2b. Two kinds of coal mining methods were adopted, namely a flexible-cover-support mining method for coal thicknesses of >1.6 m and a long-wall-sublevel dense mining method for coal thicknesses of <1.6 m. When the flexible-cover-support method was adopted, the roadway slope of the working face was arranged in sections of 23~25° in the stage.

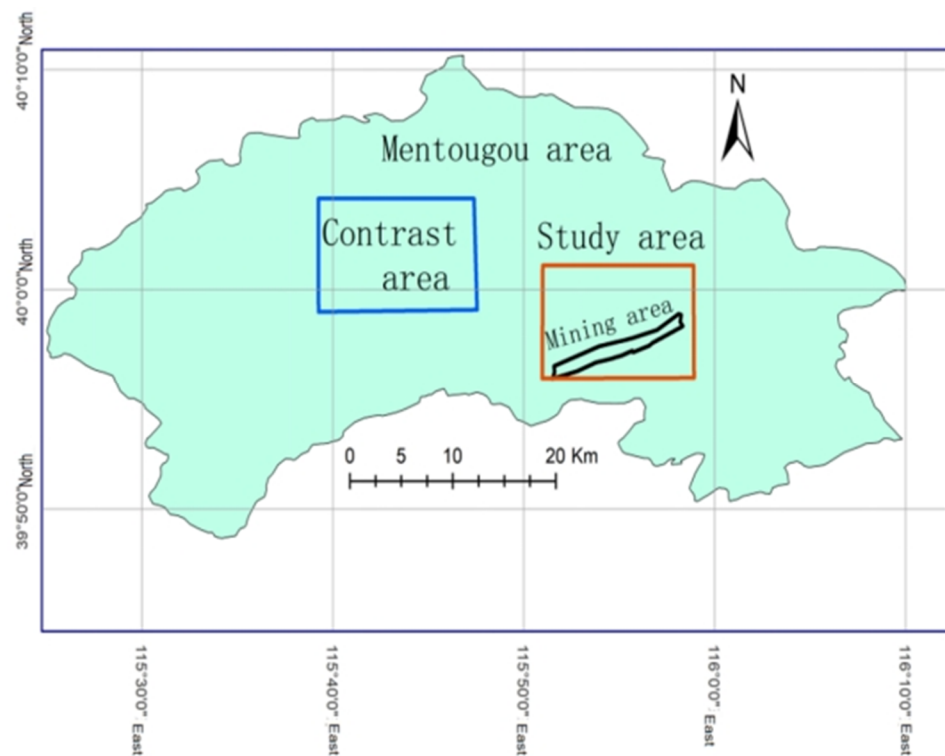


Figure 1. Location map of the study area, contrast area, and Mentougou District of Datai Mine.

The climatic condition of the Datai mining area is a warm–temperate, semi-humid, semi-arid monsoon continental climate. There are four distinct seasons: dry winter, windy spring, little rain, rainy summer, and sunny and mild autumn.

The vegetation type in the Datai Mine is that of a warm–temperate, deciduous broad-leaved forest, and the available forest land is shrub forest or mixed forest (Figure 2c). Forest vegetation is mainly distributed in Zhongshan Mountains above 1000 m above sea level (Figure 2d). In the low mountainous areas below 1000 m above sea level, vegetation is severely damaged due to frequent human activities.

The problems related to the geological environment in this mining area mainly manifest as land occupation, topographic and landform damage, gangue mountain collapse, thin soil layers, and severe soil erosion. Therefore, we selected the Datai Mine in western Beijing as our research object, and in this paper, we discuss the various characteristics of its vegetation NPP based on the situation of artificial restoration after the environment of the mining area is damaged.

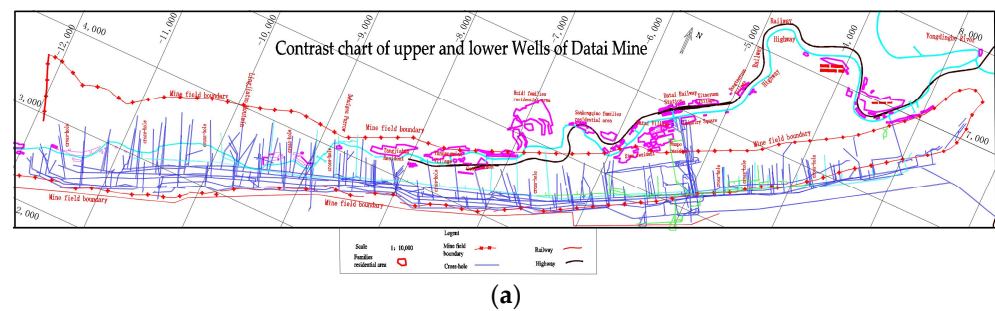


Figure 2. Cont.

analysis of the data and the background value of the file were also carried out. Finally, the resulting data were converted into a file format consistent with that of the meteorological data.

- (3) The NDVI data were derived from the geographic data cloud platform. We selected Landsat TM products within the study area with a spatial resolution of 30 m. First of all, it is necessary to carry out the radiometric calibration and atmospheric correction of the NDVI; then, use the formula calculate the NDVI and extract by mask with the study area; finally, a file with the meteorological data was generated. The results images are shown in Figure 3a,b.

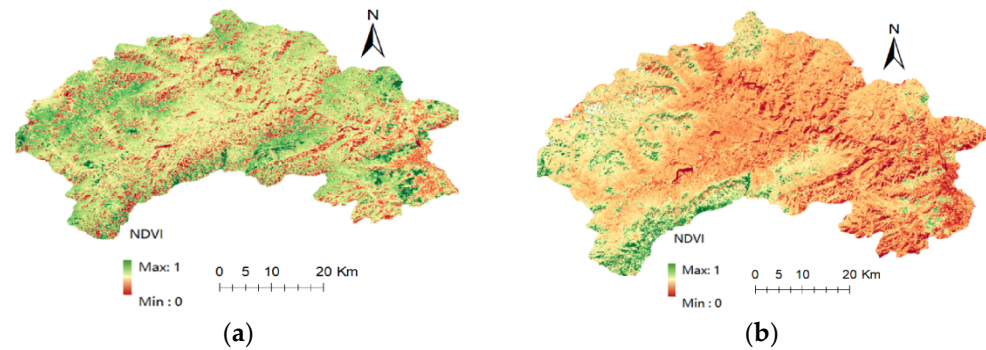


Figure 3. (a) The NDVI of Mentougou District in 2013; (b) the NDVI of Mentougou District in 2017.

2.4. Calculation of Net Primary Productivity

As the study area is located on a mountainous landform, the regional scale is small, the vegetation type in the area is of a single type, and its distribution is uneven. In this paper, we used the improved CASA model and its related software to calculate the net primary productivity of vegetation [26]. In the formula, $NPP(x,t)$ is the net primary productivity of pixel x in the t period. The absorbed photosynthetic active radiation (APAR) by plants and the actual light energy utilization rate (ϵ) are two critical factors representing the vegetation NPP [27–29]:

$$NPP(x,t) = APAR(x,t) \times \epsilon(x,t) \quad (1)$$

where $APAR(x,t)$ is the photosynthetically active radiation (gC/m^2) absorbed by pixel x in the t period, and its formula is as follows:

$$APAR(x,t) = SOL(x,t) \times FPAP(x,t) \times 0.5 \quad (2)$$

In the above formula, $SOL(x,t)$ is the total solar radiation absorbed by pixel x in the t period (MJ/m^2), and $FPAP(x,t)$ is the absorption ratio of the incident photosynthetically active radiation by the vegetation layer. The constant 0.5 is the photosynthetically active radiation used by the vegetation layer to account for the total solar radiation. In $FPAP(x,t)$, the normalized difference vegetation index (NDVI) and the simple ratio index (SR) have an excellent linear relationship; thus, combining the two factors can improve the calculation accuracy. The calculation of a pixel's $FPAP$ value can be found in the studies of Chen [30,31].

In addition, $\epsilon(x,t)$ is the actual light energy utilization (gC/MJ) of pixel x in the t period, and its formula is as follows:

$$\epsilon(x,t) = T\epsilon1(x,t) \times T\epsilon2(x,t) \times W\epsilon(x,t) \times \epsilon_{max} \quad (3)$$

In the above formula, $T\epsilon1(x,t)$ and $T\epsilon2(x,t)$ are the stress effects of low temperature and high temperature on the light energy utilization rate, respectively; $W\epsilon(x,t)$ is the water stress influence coefficient; and ϵ_{max} is the maximum light energy utilization rate (gC/MJ) under the ideal condition of surface vegetation.

2.5. Trend Analysis of NPP

The trend analysis method based on univariate linear regression was used to analyze the inter-annual NPP from 2013 to 2021 [32]. The calculation formula is as follows:

$$K_{\text{slope}} = \frac{n \times \sum_{i=1}^n (i \times \text{NPP}_i) - \sum_{i=1}^n i \times \sum_{i=1}^n \text{NPP}_i}{n \sum_{i=1}^n i^2 - (\sum_{i=1}^n i)^2} \quad (4)$$

In this formula, K_{slope} is the linear slope, NPP_i is the annual total net primary productivity in the i th year, and n is 9. When $K_{\text{slope}} > 0$, it means that the NPP is increasing over time; otherwise, the NPP is decreasing.

2.6. Correlation Analysis of NPP and Meteorological Factors

Based on the correlation coefficient between the net primary productivity of vegetation and meteorological factors (temperature, precipitation, and solar radiation), the formula is [33]:

$$\rho_{xy} = \frac{\sum_{i=1}^n [(x_i - \bar{x})(y_i - \bar{y})]}{\sqrt{\sum_{i=1}^n (x_i - \bar{x})^2 \sum_{i=1}^n (y_i - \bar{y})^2}} \quad (5)$$

In the above formula, ρ_{xy} is the correlation coefficient of the two variables; n is 9; x_i and y_i are the NPP value and the meteorological value of the two variables in the i th year; and \bar{x} and \bar{y} are the mean values of the two, respectively.

2.7. Fitting Relationship between NPP and Meteorological Factors

In order to further study the gradient relationship between the vegetation NPP and meteorological factors, in this section, we used the Origin software to construct a nonlinear curve model based on the principle of least squares. By fitting 21 functional formulas, the maximum value of R^2 was selected as the relationship between the vegetation NPP and climatic factors. As shown in Table 1, five functions were selected as representatives, which are listed along with their relevant goodness of fit.

Table 1. Fitting coefficient table of NPP and meteorological factors.

Function/ R^2	Boltzmann Function	Gaussian Function	Logistic Function	Sine Function	Exponential Function
NPP1 (T)	0.98	0.95	0.04	0.96	0
NPP2 (P)	0.78	0.80	0.76	0.73	0.79
NPP3 (R)	0.73	0.75	0.73	0.72	0

(1) The Boltzmann fitting of the NPP and temperature (T):

$$DI_NPP1(T) = \frac{A_1 - A_2}{1 + e^{(T-T_0)/dx}} + A_2 \quad (6)$$

In this formula, A_1 is the minimum value of the Boltzmann function; A_2 is the maximum value of the function; $T_0 = (A_1 + A_2)/2$; and dx is the time period.

(2) The Gaussian fitting of the NPP and precipitation (P):

$$DI_NPP2(P) = \frac{A}{w\sqrt{\pi/2}} e^{-\frac{2(P-P_c)^2}{w^2}} + P_0 \quad (7)$$

In the above formula, P_0 is the minimum value of the Gaussian function; $A/w\sqrt{(\pi/2)}$ is the function peak; P_c is its corresponding abscissa; and W is the standard deviation.

(3) The Gaussian fitting of the NPP and radiation (R):

$$DI_NPP3(R) = \frac{A}{w\sqrt{\pi/2}} e^{-\frac{2(R-R_c)^2}{w^2}} + R_0 \quad (8)$$

In this formula, R_0 is the minimum value of the Gaussian function; $A/w\sqrt{(\pi/2)}$ is the function peak; R_c is its corresponding abscissa; and W is the standard deviation.

3. Result and Analysis

3.1. The Analysis of Time Series Variation Characteristics of NPP in the Study Area

3.1.1. The Monthly Variation Characteristics of NPP of Vegetation in the Study Area

Figure 4 indicates that the monthly average vegetation NPP had a change in trend in the Mentougou District, the Datai Mine research area, and the control area from 2013 to 2021. From the 9-year data, it can be found that the monthly average value of the net primary productivity of vegetation in the study area of the Datai Mine was 11.4% higher than that in the control area. The NPP of vegetation in the three areas rapidly increased from April and reached the peak carbon sequestration capacity from June to August. The maximum value range in the research area of the Datai Mine was 110.8–124.7 gC/m^2 , which is basically unchanged.

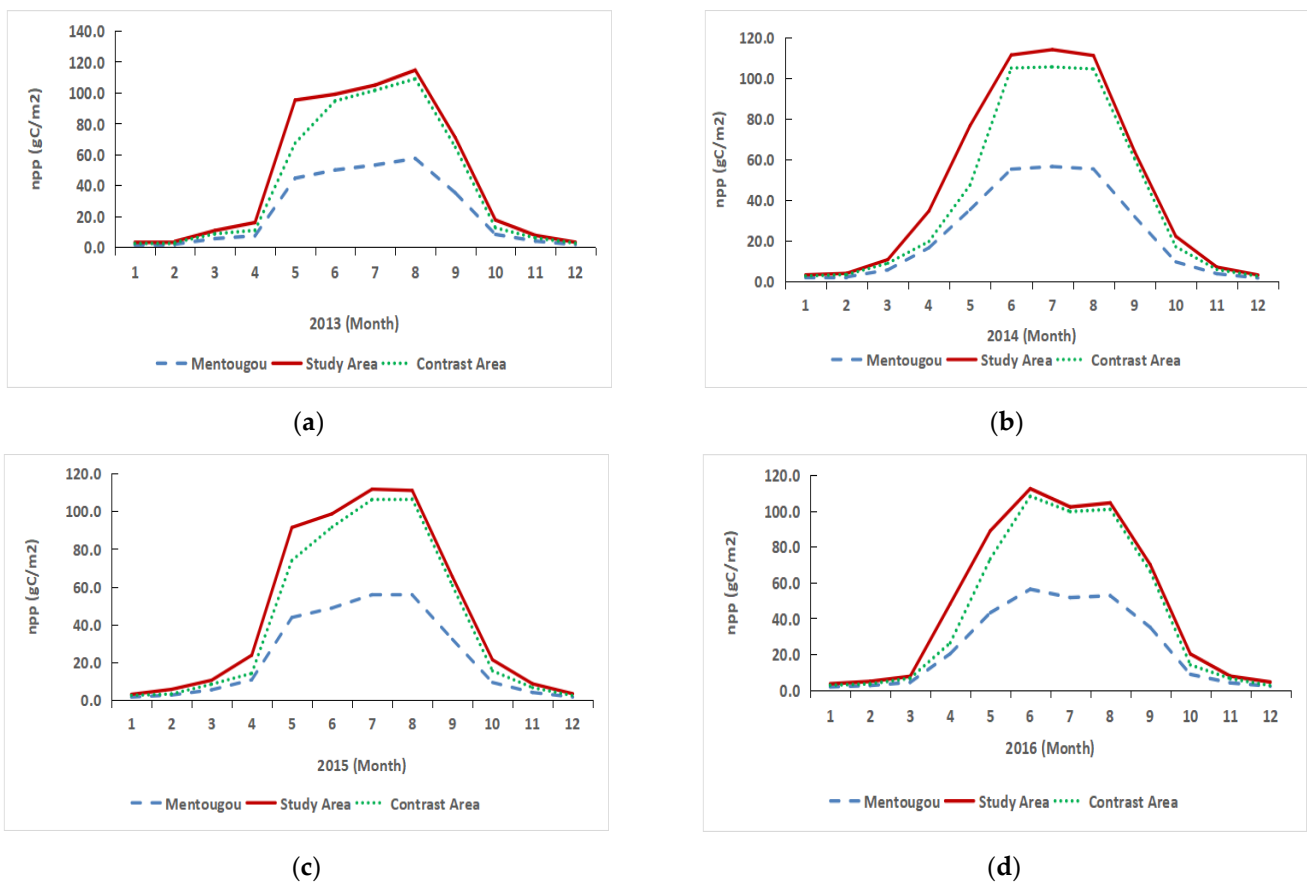


Figure 4. Cont.

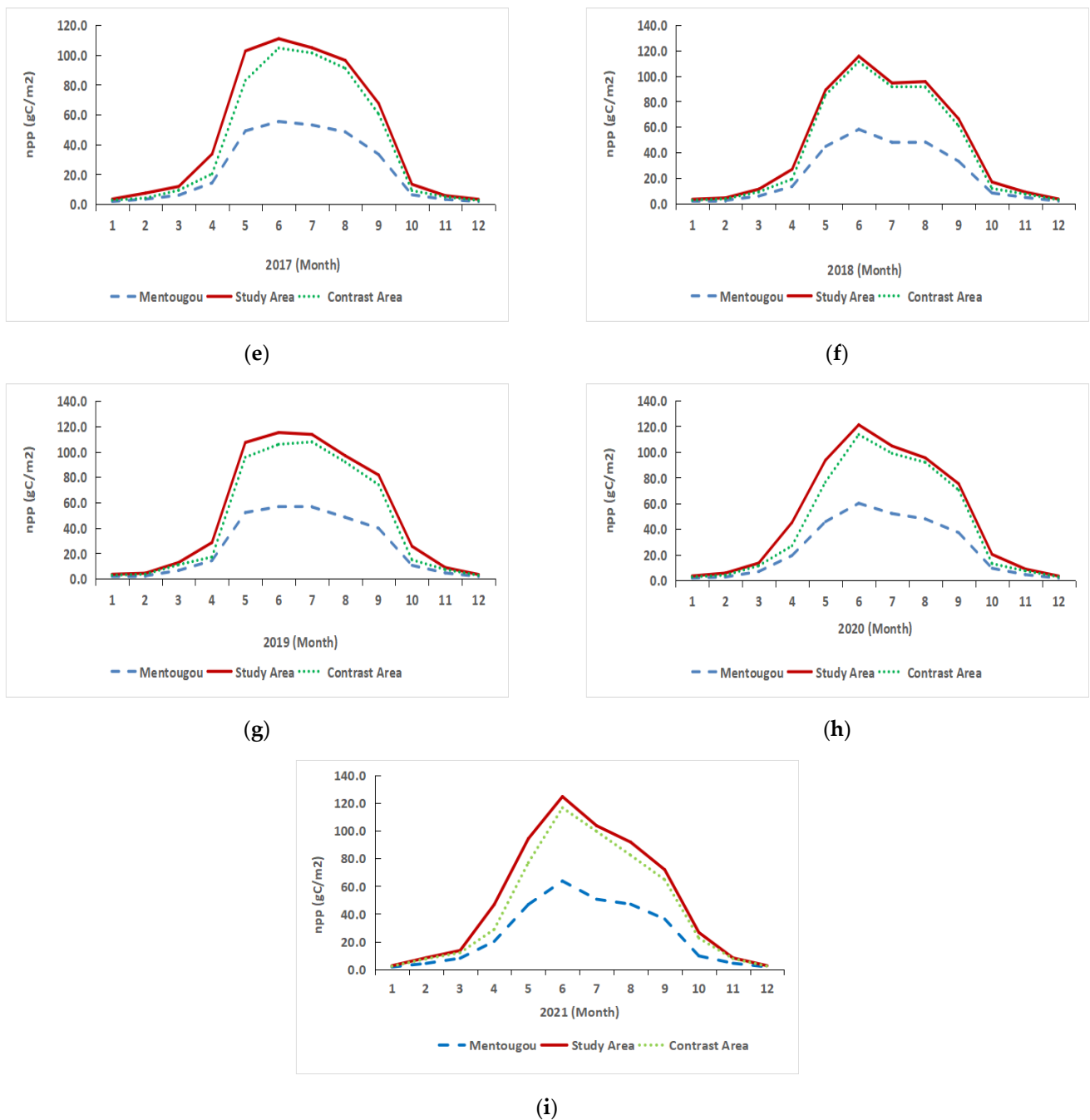


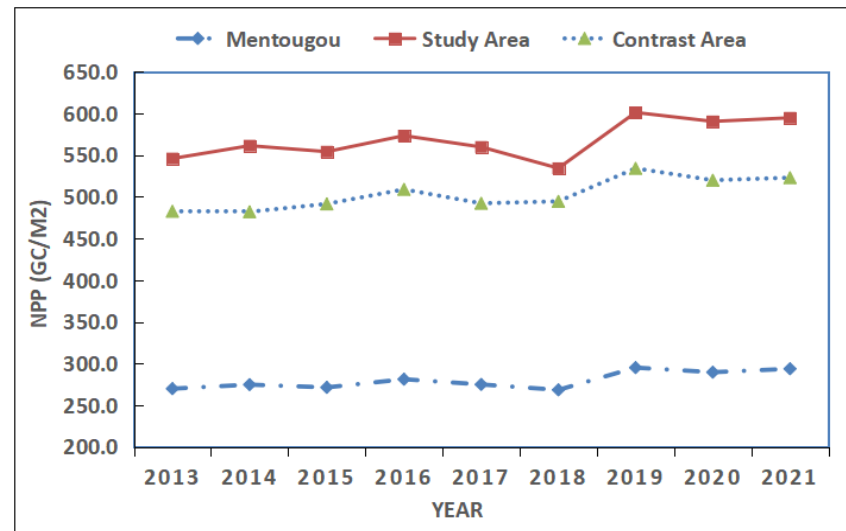
Figure 4. Comparison of monthly average vegetation NPP from 2013 to 2021. (a–i) are the represent data from 2013 to 2021 respectively.

In conclusion, the variation characteristics of the vegetation NPP in these three regions were the same each year; the monthly average value of the vegetation NPP in the Datai Mine study area and the control area was relatively close. The changing trend of the vegetation NPP in the Mentougou District was relatively flat.

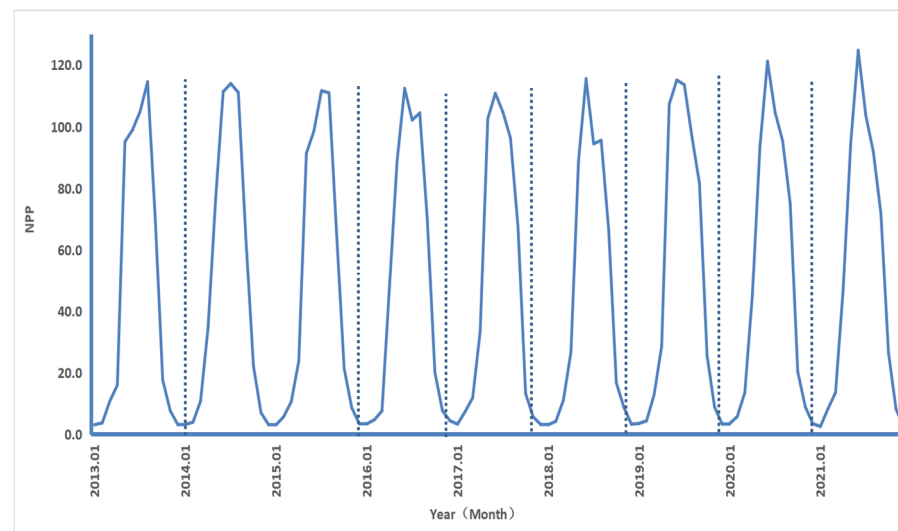
3.1.2. The Annual Characteristics of NPP of Vegetation in the Study Area

According to the changing trend in Figure 5a, although the vegetation NPP in the control area slightly decreased from 2013 to 2014 and slightly increased from 2017 to 2018, they all reached their peaks in 2019. The year-on-year increases were 10%, 12.5%, and 8% in the study area, the control area, and the Mentougou District. In 2019, the vegetation NPP

in the three regions became the highest value, while the lowest value in the control area and other areas were in 2014 and 2018 respectively.



(a)



(b)

Figure 5. (a) The curve of annual average vegetation NPP from 2013 to 2021; (b) the annual variation characteristics of vegetation NPP from 2013 to 2021.

In conclusion, the variation characteristics of the average annual vegetation NPP in the three areas were the same. From the average annual change, it can be concluded that the mining operations in the Datai mining area in western Beijing had no significant impact on the surrounding environment. The annual average vegetation NPP in the study area was always higher than that of other areas, and the changing trend tended to be consistent, indicating that the efforts toward the environmental restoration and management of the Datai mining area are currently not significant.

Figure 5b shows the annual temporal change characteristics of the vegetation NPP in the Datai study area from 2013 to 2021. It can be seen from the figure that the vegetation NPP first increased and then decreased throughout each year, and the maximum value was concentrated in June (2016–2021); the maximum value in 2014–2015 was found in July; and only in 2013, the maximum value was in August.

3.2. Spatial Variation Characteristics of Vegetation NPP in the Mentougou District

Based on the CASA model, the distribution characteristics of the vegetation NPP in the Mentougou District from 2013 to 2021 were calculated, as shown in Figure 6. The maximum and minimum NPP values were 447 gC/m² and 402 gC/m² in the years 2021 and 2018, respectively. The low value of the NPP was concentrated in the eastern area but generally improved over the 9 years under study.

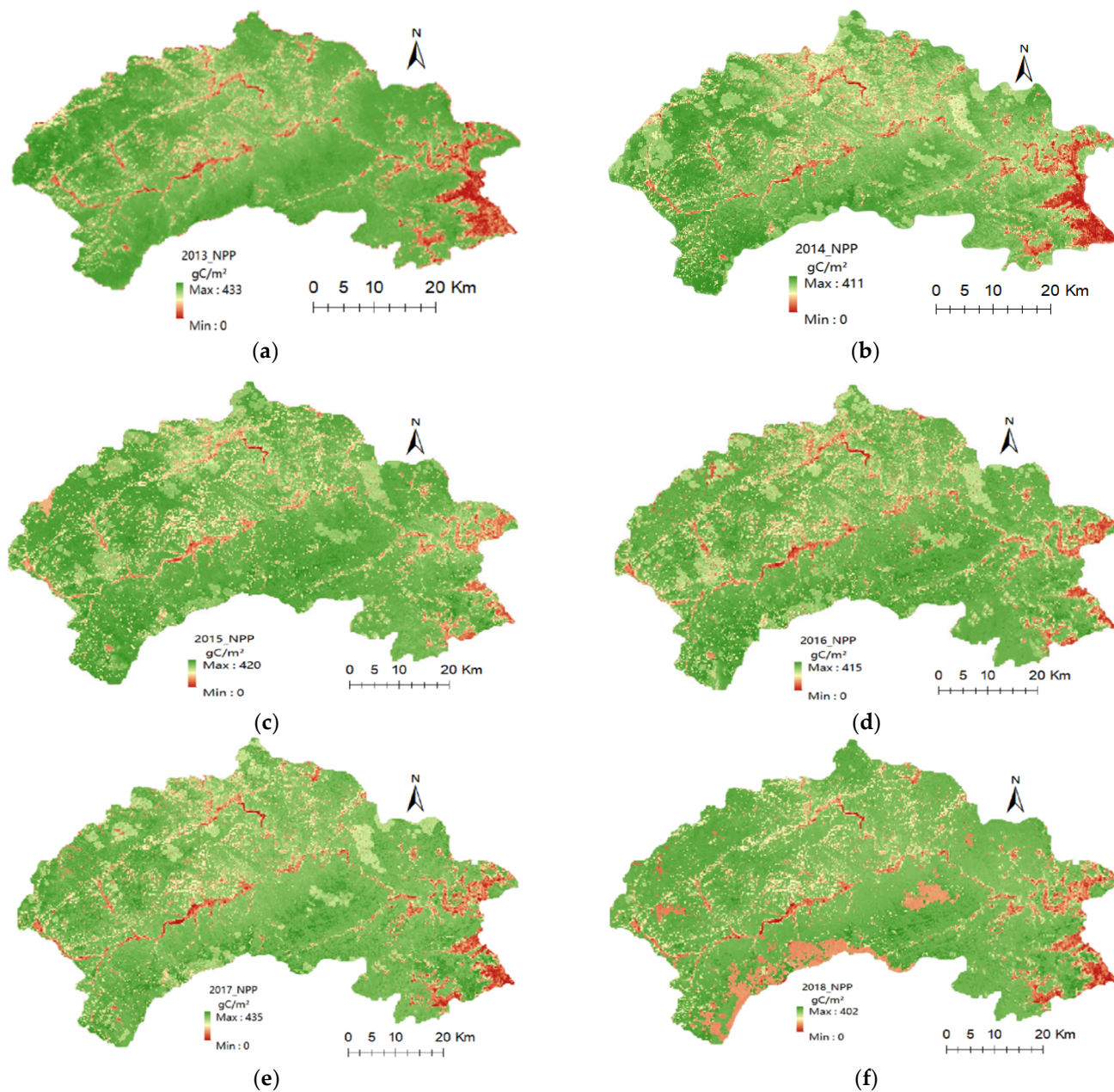


Figure 6. Cont.

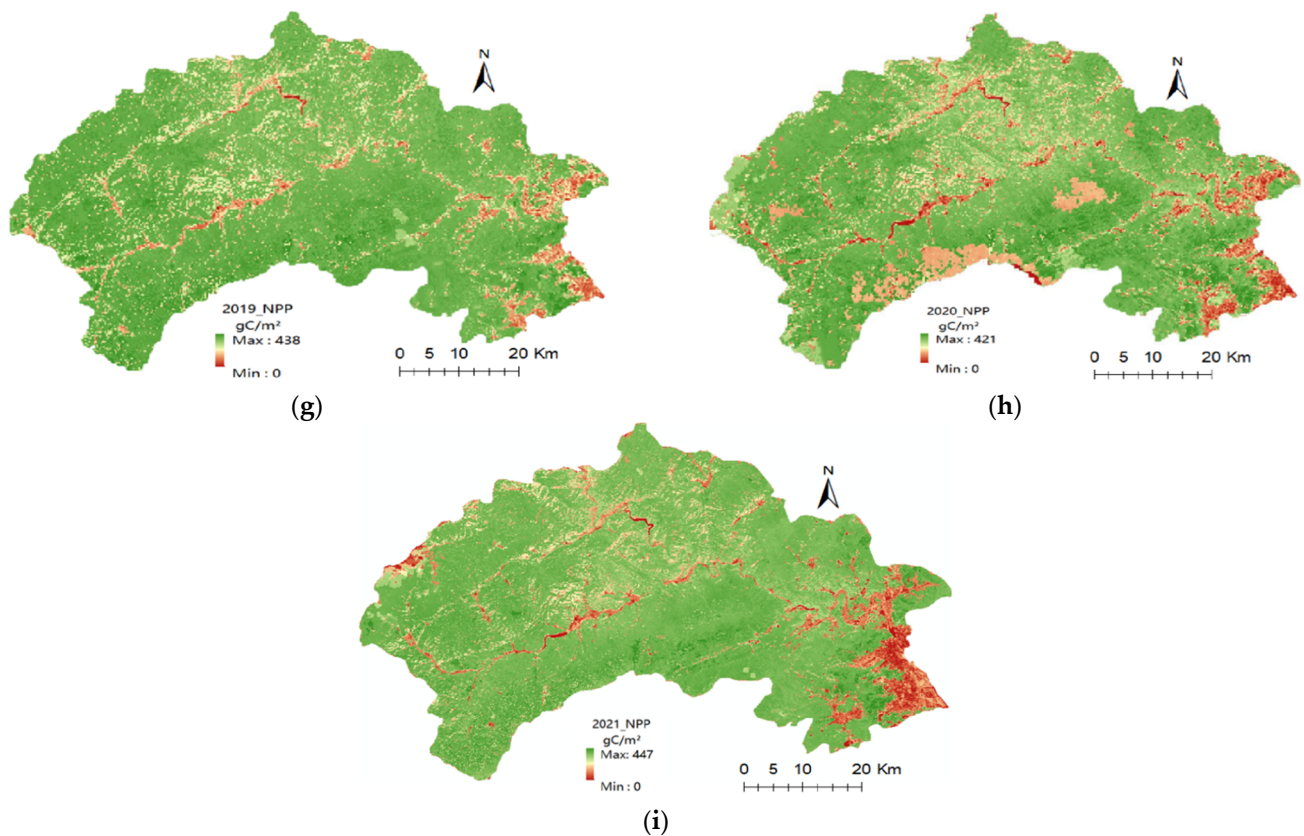


Figure 6. Spatial distribution of vegetation NPP in Mentougou District from 2013 to 2021. (a–i) are the represent data from 2013 to 2021 respectively.

From the spatial distribution figure of the vegetation NPP in the Mentougou District from 2013 to 2021, it can be seen that the NPP in the eastern region was lower than that of the other regions. This is because the eastern region is located in an industrial development zone, and its pollution has had a significant impact on the environment, indicated by the red color in some areas, while the population of the Mentougou District is concentrated in the central area, which has also a certain impact on the environment, and it is indicated in pale yellow on the spatial distribution figure; since the southwest area mostly covers scenic spots and nature reserves, its NPP value was mostly higher than the other areas. The highest NPP values were mostly distributed in the Shuanglong Gorge Scenic Area and the Baihua Mountain Nature Reserve.

After performing the univariate linear regression analysis to determine the pixel-by-pixel variation trend of the vegetation NPP in the Mentougou District over the past 9 years, as shown in Figure 7a, it was found that in 30% of the area, the linear slope of the NPP was less than 0. The rate of change from a significant decrease to a significant increase was 9–21–50–17–3%. The figure displays that most areas of the Mentougou District showed a trend of stability and decline over the 9 years, the NPP of the whole area gradually increased from south to north, and the areas with a significant increase in the vegetation NPP were concentrated in the eastern and northern parts.

Based on the grading map of the average vegetation NPP value in the Mentougou District from 2013 to 2021 (Figure 7b), it can be seen that 11% of the area had a vegetation NPP value of 0–75 gC/m^2 , 16% of the area had a vegetation NPP value of 75–200 gC/m^2 , 16% of the regional vegetation NPP value was 200–300 gC/m^2 , 24% of the regional vegetation NPP value was 300–600 gC/m^2 , and 33% of the regional vegetation NPP value was between 600 and 700 gC/m^2 .

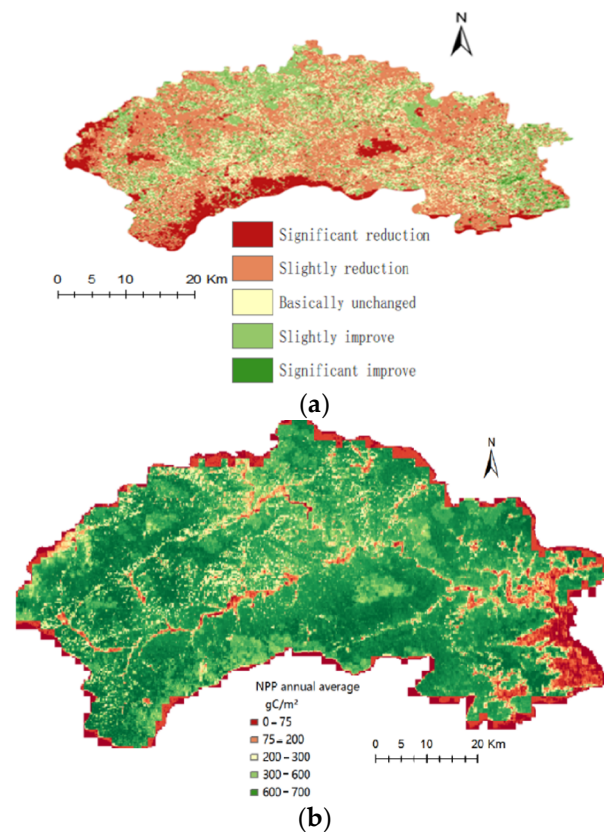


Figure 7. (a) Variation trend of annual average NPP in Mentougou District; (b) the spatial distribution of annual average NPP in Mentougou District.

3.3. Analysis of Meteorological Driving Factors of Vegetation NPP in the Datai Mine Study Area

3.3.1. Temporal Analysis of Vegetation NPP and Meteorological Factors in the Study Area of Datai Mine

(1) The relationship between vegetation NPP and temperature (T)

From the monthly vegetation NPP sample data and the corresponding monthly average temperature, the change in the vegetation NPP showed a law of slowly increasing, sharply increasing, and then slowly increasing, so the Boltzmann function was used for fitting. Figure 8a shows the Boltzmann fitting curve of the 9-year monthly vegetation NPP value and the monthly average temperature (T). The gradient relationship between the NPP and temperature (10) is shown in Figure 8b with the vegetation NPP–T gradient curve; the temperature value interval $T \in [-5.6, 25.8]$, °C.

$$NPP1(T) = \frac{-110}{1 + e^{(T-17.6)/2.7}} + 115 \quad (9)$$

$$k_T(T) = \frac{40.7e^{(T-17.6)/2.7}}{[1 + e^{(T-17.6)/2.7}]^2} \quad (10)$$

where $NPP1(T)$ is the fitting function of the monthly vegetation net primary productivity and the monthly average temperature, gC/m^2 ; T is the monthly average temperature, °C; the $k_T(T)$ is the variation gradient of the monthly vegetation NPP with respect to the temperature.

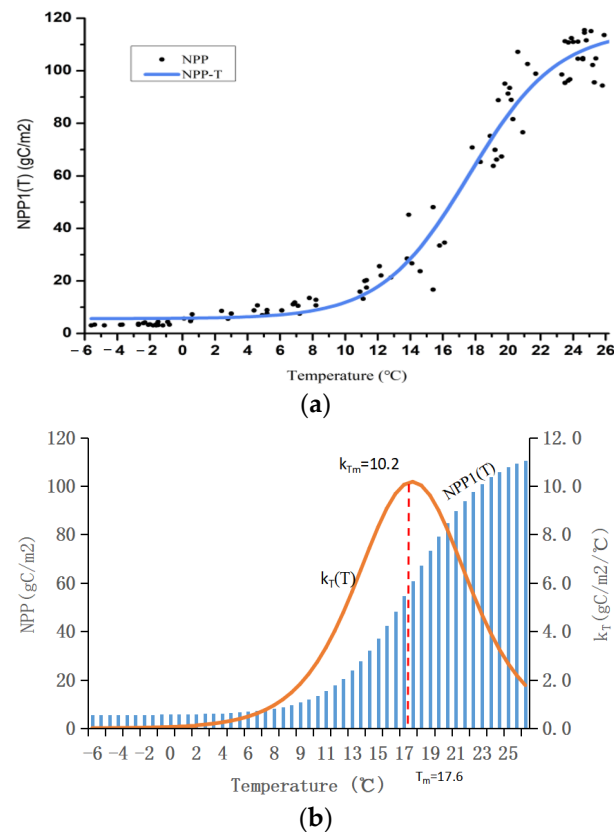


Figure 8. (a) The relationship between vegetation NPP and temperature in the study area; (b) the gradient of vegetation NPP with respect to temperature.

The R^2 of the fitting function $NPP1(T)$ was 0.97, indicating that there was a positive fitting relationship between the two factors. It can be seen from the vegetation NPP temperature increase gradient that the extreme value point of $K_T(T)$ was $T_m = 17.6$ °C, when $T \in [-5.6, 17.6]$, the growth rate of the vegetation NPP increased with the increase in temperature; $T \in [17.6, 25.8]$, and the growth rate of the vegetation NPP decreased with the increase in temperature.

(2) The relationship between NPP of vegetation and precipitation (P)

With the increase in precipitation, the change in the vegetation NPP showed a continuous growth–maintained stability law, so the Gaussian function was used for fitting. Figure 9a is the Gaussian fitting curve of the monthly vegetation NPP value and the monthly average precipitation (P) for the 9 years. The gradient relationship between the vegetation NPP and precipitation (12) is shown in Figure 9b with the vegetation NPP–P gradient curve; the precipitation value interval $P \in [0, 331.8]$, mm.

$$NPP2(P) = 101.1(1 - e^{-2\frac{(P+9.2)^2}{3474.2}}) \quad (11)$$

$$k_P(P) = 0.12(P + 9.2)e^{-2\frac{(P+9.2)^2}{3474.2}} \quad (12)$$

where $NPP2(P)$ is the fitting function of the monthly vegetation net primary productivity and the monthly average precipitation, gC/m^2 ; P is the monthly average precipitation, mm; $k_P(P)$ is the variation gradient of the monthly vegetation NPP with respect to precipitation.

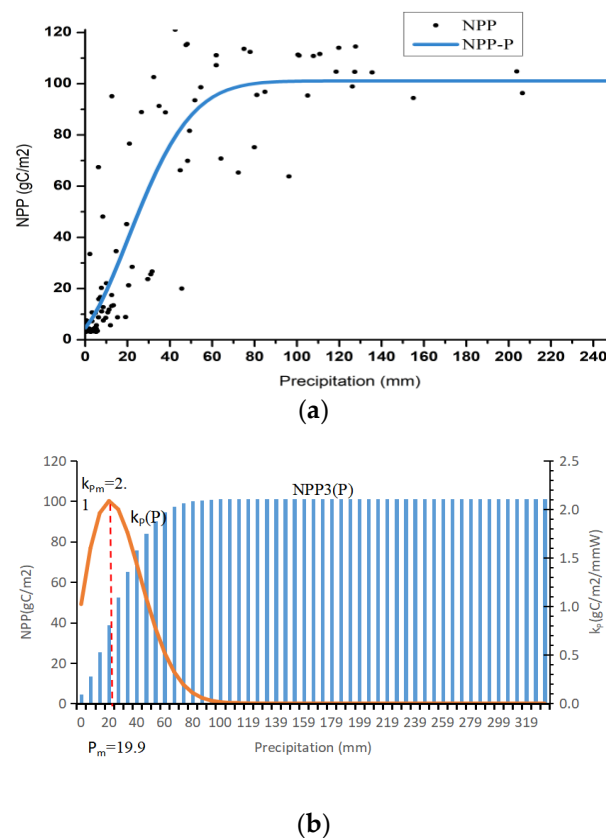


Figure 9. (a) Relationship between vegetation NPP and precipitation in the study area; (b) variation gradient of vegetation NPP with respect to precipitation.

The R^2 of the fitting function $NPP2(P)$ was 0.80, which indicates that there was a positive fitting relationship between the two factors. It can be seen from the NPP precipitation gradient that the point is the P_m extreme point of fitting the NPP–P function; that is, when $P \in [0, 2.1]$, the growth rate of the vegetation NPP increases with the increase in precipitation; when $P \in [2.1, 331.8]$, the growth rate of the vegetation NPP decreased with the increase in precipitation, and the growth was suspended until the precipitation was 101.08 mm.

(3) Relationship between vegetation NPP and solar radiation (R)

With the increase in solar radiation, the change in the vegetation NPP showed a trending law of first decreasing and then a continuous increase, so the Gaussian function was used for fitting. Figure 10a is the Gaussian fitting curve of the monthly vegetation NPP value and the monthly average solar radiation (R) for the 9 years. The gradient relationship between the vegetation NPP and precipitation (14) is shown in Figure 10b, with the vegetation NPP–P gradient curve; the value range of solar radiation is $R \in [0, 719.8]$, MJ/m².

$$NPP3(R) = 123.2 - 121.2e^{-2\frac{(R-308.9)^2}{395.5}} \quad (13)$$

$$k_R(R) = 0.003(R - 308.9)e^{-2\frac{(R-308.9)^2}{395.5}} \quad (14)$$

where $NPP3(R)$ is the monthly net primary productivity of vegetation and the monthly average solar radiation fitting function, gC/m²; R is the monthly average solar radiation, MJ/m²; $k_R(R)$ is the monthly variation gradient of the vegetation NPP with respect to solar radiation.

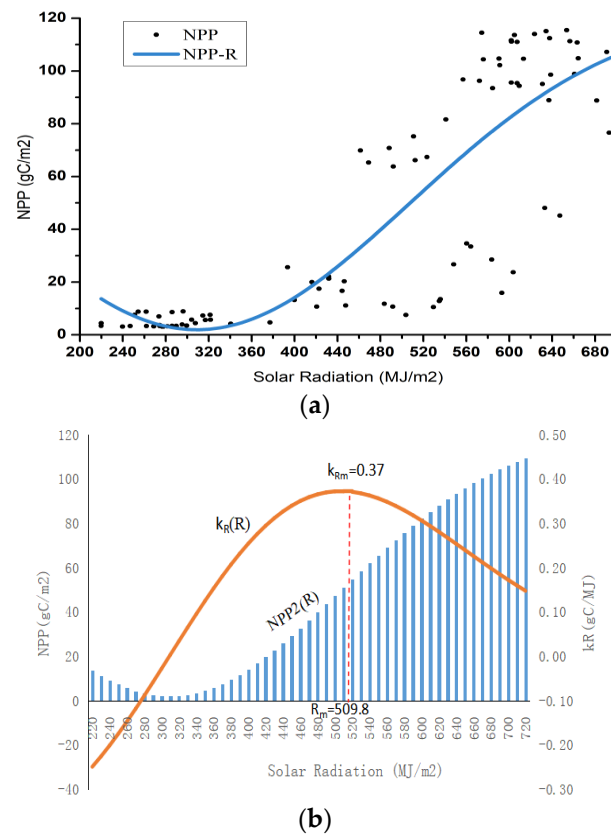


Figure 10. (a) Relationship between vegetation NPP and solar radiation in the study area; (b) variation gradient of vegetation NPP with respect to solar radiation.

The R^2 of the fitting function $NPP3(R)$ was 0.75, which indicates that there was a positive fitting relationship between the two factors. From the data for the vegetation NPP solar radiation gradient, it can be seen that the point was the R_m extreme point of fitting the $NPP-R$ function; that is, when $R \in [219.8, 509.8]$, the vegetation NPP growth rate increased with the increase in solar radiation; when $R \in [509.8, 719.8]$, the growth rate of the vegetation NPP decreased with the increase in solar radiation.

3.3.2. Multivariate Analysis of Vegetation NPP and Meteorological and Mining Factors in the Mentougou District

Considering the factors of climatic, the Datai mining area (for example: ground surface settlement), and human intervention, this section summarizes the data of the maximum ground surface settlement (GSS), coal production (CP), artificial restoration cost (ARC), meteorological factors, and the vegetation NPP of the Datai Mine from 2013 to 2021.

The GSS data were derived from the deformation monitoring summary report of the Datai Mine from 2013 to 2021, and the ARC data were derived from the “Design Plan of Geological Environment Treatment Project for Waste Dumps Subsidence Pits of Datai Coal Mine” and the “Geological Environment Protection and Land Reclamation Plan for Datai Coal Mine in West Beijing”. Since the Datai Mine was closed on 17 September 2019, its coal output from 2020 to 2021 was zero.

In order to eliminate the limitation of the units and magnitudes of the different factors’ data, we considered the meteorological factors and the vegetation NPP data as dimensionless numbers (DNs). The maximum values of the vegetation NPP data and each meteorological observation factor’s monthly average data derived from the Datai Meteorological Station are shown in Table 2.

Table 2. The monthly average maximum values of vegetation NPP and meteorological and mining area factors from 2013 to 2021.

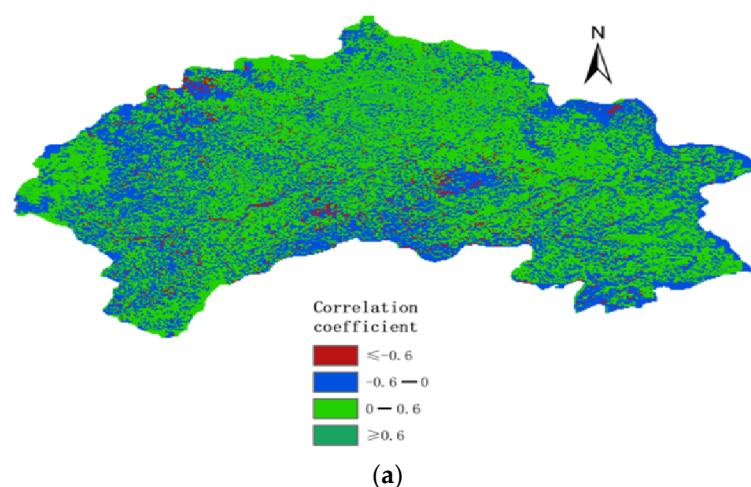
Year	NPP _{max} (gC/m ²)	T _{max} (°C)	P _{max} (mm)	R _{max} (MJ/m ²)	GSS (mm)	CP (kt)	ARC (kcnny)
2013	114.5	24.7	203.8	664.4	7.2	903	0
2014	114.0	26.7	119.8	693.1	16.8	898	3515
2015	111.6	24.8	110.8	716.7	18.1	933	0
2016	112.4	25.2	331.8	681.5	20.2	840	0
2017	110.8	25.4	206.5	719.7	21.5	933	7659
2018	111.5	25.8	155	653.6	45.7	1000	0
2019	115.1	25.9	84.9	690.9	48.5	361	7250
2020	121.1	25.7	127.3	647.2	30.2	0	0
2021	124.7	24.6	308.5	683.4	37.6	0	0

After fitting the vegetation NPP with the maximum surface subsidence, the coal yield, and artificial restoration costs, it was found that the correction determination coefficient (R^2_{adjusted}) was 0.87, indicating a high fitting degree. It can be seen from the fitting results of the characteristics of low-intensity mining areas that among meteorological factors, the temperature was the main factor affecting the changes in the NPP of vegetation, and the impacts of the mining area and human intervention are secondary factors. The dimensionless fitting results are as follows:

$$DI_NPP(CP, GSS, ARC, T, P, R) = -0.03 - 0.004 CP - 0.003 GSS + 0.0001 ARC + 0.69T + 0.37P + 0.14R \quad (15)$$

3.3.3. Spatial Analysis of Vegetation NPP and Meteorological Factors in the Mentougou District

Climate change has a direct impact on the type, structure, distribution, and function of vegetation [2]. In this paper, the correlation coefficients between the vegetation NPP and the air temperature, precipitation, and solar radiation in the 9 years were calculated from the pixel scale (Figure 11). The results show that the annual vegetation NPP change had little relationship with the fluctuation of the annual average temperature and solar radiation and overall insignificant positive and negative correlations, respectively. However, the annual vegetation NPP change in the Mentougou District had a relatively large correlation with the annual precipitation change, the grassland area was positively correlated with more than 70%, and the correlation coefficient between the two was up to 0.96.

**Figure 11.** Cont.

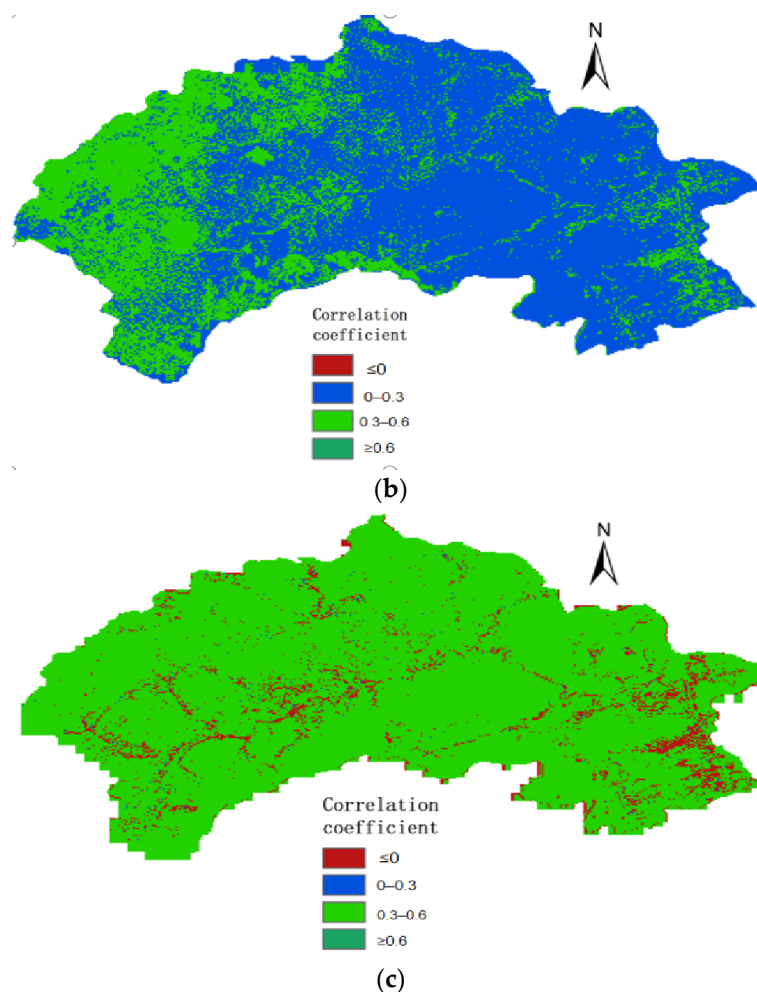


Figure 11. Spatial distributions of the correlation coefficient (a) between annual NPP and annual cumulative precipitation; (b) between annual NPP and annual mean temperature; and (c) between annual NPP and solar radiation.

4. Discussion

There are fewer studies on the spatial and temporal characteristics of the NPP in Mentougou. The NPP results of the MODIS–NPP data used in the CASA model are basically consistent with the findings of this article [34,35]. Considering the NPP results in Beijing, some studies also provide the changing trend of the NPP, the results of which are consistent with those found in this article [36,37], which means that the NPP in the Mentougou District displayed a trend of fluctuating rise from 2013 to 2020. Limited by the Landsat 8 data, in this article, we only analyzed the NPP spatiotemporal characteristics of high-precision remote sensing images since 2013. Whether the ecological restoration project of the coal mine will lead to a significant impact of NPP on coal production, surface subsidence and restoration projects remains to be further studied.

Moreover, an increasing number of studies are interested in the lag between climatic elements and the NPP [38,39]. Therefore, in further research, we will select the CASA model and combine the data from multiple sources to compare the long-term period NPP in coal mining and analyze the time lag between the NPP and meteorological factors.

When studying the effect of climatic factors (temperature, precipitation, and solar radiation) on the NPP, most studies have proved that the NPP changes are crucially impacted by precipitation [40,41], which is consistent with this article. Some studies, however, revealed that the NPP changes are affected by precipitation and temperature [42,43]. The reasons for such different results are the various databases or different research cycles considered in these studies.

5. Conclusions

Based on the meteorological data of a mining area and the remote sensing images of land use types, we used the improved CASA model to calculate the net primary productivity (NPP) of vegetation in the Datai Mine study area, the control area, and the Mentougou District from 2013 to 2021. The spatial variation in the NPP was analyzed through a hierarchical process, and the relationship between the NPP on meteorological factors and mining area factors was discussed.

- (1) We analyzed the data and found that the vegetation carbon sequestration capacity in the research area of the Datai Mine changed at a consistent and gradual annual rate; in addition, it was revealed that the NPP of vegetation in the Datai Mine study area covered an annual cycle and gradually increased first, then rapidly increased, reaching a peak value, and then sharply to slowly decreased.
- (2) The results showed that the changing trend of the NPP value of vegetation in the study area and the comparison area of the Datai Mine was consistent, which confirmed that under the low-intensity mining conditions of the Datai Mine, mining operations had no significant impact on the carbon sequestration of vegetation. This conclusion is applicable to low-intensity mining areas with a similar topographic environment, vegetation characteristics, and climatic conditions.
- (3) Based on the observation data of the Datai Meteorological Station, the fitting relationship and variation gradient of the temperature, precipitation, solar radiation, and vegetation NPP in the study area were analyzed and obtained. When the temperature was 17.6 °C, the precipitation was 101.08 mm, and the solar radiation was 509.8 MJ/m², the vegetation NPP reached its maximum value. Further studies are needed to analyze the comprehensive impact of these multiple factors on the NPP.
- (4) Among the meteorological factors that affect the change of NPP in Mentougou area, the correlation with NPP is from large to small for precipitation, temperature and solar radiation. Precipitation was the main meteorological factor that affected the change in the NPP.
- (5) There are still some deficiencies in this study that need to be improved. First, when acquiring the data from the meteorological station, a few meteorological observation stations had missing data for some daily periods. Therefore, we used the data from the adjacent meteorological stations to supplement (such as the daily temperature or precipitation). Second, the factors influencing the vegetation NPP are not only environmental factors but also vegetation characteristics and human activities, which affect the changes in the vegetation NPP. Additionally, further studies should also combine the coal output, ground surface settlement, and some mining elements in their analysis. Moreover, the fluctuation of NPP in coal mines is affected by climate change, the results of recovery projects and mining factors. Meanwhile, the process of restoration projects and the influence of mining factors have no obvious regularity. Thus, combined with climatic factors, it is hard to distinguish which area is dominated by these different impact factors. In future research, we will build an integrated computational model of the coal mining NPP based on meteorological and mining elements to analyze the impact of these various factors on the NPP.

Author Contributions: Conceptualization, L.D. and Y.Z.; methodology, L.D. and Y.Y.; software, R.D. and Y.Z.; validation, R.D. and Y.Z.; formal analysis, L.D. and Y.Z.; writing—original draft preparation, R.D. and Y.Y.; writing—review and editing; L.D. and Y.Z. All authors have read and agreed to the published version of the manuscript.

Funding: This work is supported by the Open Fund of the State Key Laboratory of Water Resource Protection and Utilization in Coal Mining (Grant No. GJNY-20-113-20); and supported by “the Fundamental Research Funds for the Central Universities (2022YQGL02)”.

Institutional Review Board Statement: Not applicable.

Informed Consent Statement: Informed consent was obtained from all subjects involved in the study.

Data Availability Statement: The data used to support the findings of this study are available from the corresponding author upon request.

Conflicts of Interest: The authors declare no conflict of interest.

References

- Xing, F.; Lu, L.; Yuanyuan, Q.; Xiang, G. The path and enlightenment of major developed economies from carbon peaking to carbon neutralization. *Res. Prog. Clim. Chang.* **2022**, 1–17.
- Chaitra, A.; Upgupta, S.; Bhatta, L.D.; Mathangi, J.; Anitha, D.S.; Sindhu, K.; Kumar, V.; Agrawal, N.K.; Murthy, M.S.R.; Qamar, F.; et al. Impact of Climate Change on Vegetation Distribution and Net Primary Productivity of Forests of Himalayan River Basins: Brahmaputra, Koshi and Indus. *Am. J. Clim. Chang.* **2018**, *7*, 271–294. [[CrossRef](#)]
- Ouyang, X.J.; Dong, X.; Wei, R.; Gong, C.; Wu, H. Spatial and temporal changes of NDVI during vegetation growth season on the Qinghai Tibet Plateau and its response to climate factors. *Res. Water Soil Conserv.* **2022**, *30*, 1–10.
- Zheng, J.; Fang, X.; Wu, S. Frontier Progress in Climate Change Research in China’s Physical Geography. *Prog. Geogr. Sci.* **2018**, *37*, 16–27.
- Jiao, K.; Gao, J.; Wu, S.; Hou, W. Research progress on the response process of vegetation activities to climate change. *J. Ecol.* **2018**, *38*, 2229–2238.
- Bayarsaikhan, S.; Mandakh, U.; Dorjsuren, A.; Batsaikhan, B.; Bao, Y.; Adiya, Z.; Myagmartseren, P. Variations of vegetation net primary productivity and its responses to climate change from 1982 to 2015 in Mongolia. *ISPRS Ann. Photogramm. Remote Sens. Spat. Inf. Sci.* **2020**, *3*, 347–353. [[CrossRef](#)]
- Mu, H.; An, S.; Chen, Y.; Xu, Y. Research on the carbon sequestration and oxygen release capacity of vegetation in coal mine subsidence reclamation area. *Shaanxi Coal* **2021**, *40*, 37–41+50.
- Zhang, M.; Guo Tao, L.K.; Huang, P.; Yu, J.; Liu, S.; Liu, Y.; Li, Y. Remote sensing estimation of rice LAI based on hyperspectral vegetation index. *J. Southwest Agric.* **2022**, 1–10. Available online: <http://kns.cnki.net/kcms/detail/51.1213.S.20220926.1605.062.html> (accessed on 18 November 2022).
- Zhang, Q.; Lv, W.; Xu, B. Research on the measurement of carbon sequestration capacity of urban green spaces in North China. *Environ. Sci.* **2021**, *47*, 41–48.
- Falahatkar, S.; Hosseini, S.M.; Mahiny, A.S.; Ayoubi, S.; Wang, S.-Q. Soil organic carbon stock as affected by land use/cover changes in the humid region of northern Iran. *J. Mt. Sci.* **2014**, *11*, 507–518. [[CrossRef](#)]
- Chen, K.; Wang, J.; He, Y.; Zhang, L. Assessment of forest carbon storage and carbon sequestration potential in key state-owned forest areas in Daxing’anling, Heilongjiang. *J. Ecol. Environ.* **2022**, *31*, 1–10.
- Li, H.; Du, J.; Tang, H. Estimation of soil organic carbon density and storage in counties based on random forests. *China Soil Fertil.* **2021**, *3*, 1–8.
- Li, Z.; Wang, X.; Xu, Y.; Wen, L.; Huang, L. Changes in net primary productivity of vegetation in Shangri La in northwest Yunnan from 1996 to 2015. *J. Ecol.* **2022**, *42*, 266–276.
- Field, C.B. Global net primary production: Combining ecology and remote sensing. *Remote Sens. Environ.* **1995**, *51*, 74–88. [[CrossRef](#)]
- Guoa, E.; Liu, X.; Zhang, J.; Wang, Y.; Wang, C.; Wang, R.; Lia, D. Assessing spatiotemporal variation of drought and its impact on maize yield in Northeast China. *J. Hydrol.* **2017**, *553*, 231–247. [[CrossRef](#)]
- Zhu, W. *Research on Remote Sensing Estimation of Net Primary Productivity of Vegetation in Terrestrial Ecosystems in China and Its Relationship with Climate Change*; Beijing Normal University: Beijing, China, 2005.
- Chena, Y.; Kelly, R.; Genet, H.; Lara, M.J.; Chipman, M.L.; McGuire, A.D.; Hu, F.S. Resilience and sensitivity of ecosystem carbon stocks to fire-regime change in Alaskan tundra. *Sci. Total Environ.* **2021**, *806*, 151482. [[CrossRef](#)]
- Running, S.W.; Coughlan, J.C. A general model of forest ecosystem process for regional applications I. Hydrologic balance, canopy gas exchange and primary production process. *Ecol. Model.* **1988**, *42*, 125–154. [[CrossRef](#)]
- Zhao, M.; Running, S.W.; Heinsch, F.A.; Nemani, R. *MODIS-Derived Terrestrial Primary Production*; Springer: Berlin/Heidelberg, Germany, 2011; Chapter 28; pp. 635–660.
- Liu, Q.; Zhang, T.; Du, M.; Gao, H.; Zhang, Q.; Sun, R. A better carbon-water flux simulation in multiple vegetation types by data assimilation. *For. Ecosyst.* **2022**, *9*, 100013. [[CrossRef](#)]
- Shan, N.; Zhang, Y.; Chen, J.M.; Ju, W.; Migliavacca, M.; Peñuelas, J.; Yang, X.; Zhang, Z.; Nelson, J.A.; Goulas, Y. A model for estimating transpiration from remotely sensed solar-induced chlorophyll fluorescence. *Remote Sens. Environ.* **2021**, *252*, 112134. [[CrossRef](#)]
- Pu, S.; Fang, J. Net primary productivity of vegetation on the Qinghai-Tibet Plateau and its temporal and spatial changes from 1982 to 1999. *J. Nat. Resour.* **2002**, *17*, 8.
- Wei, W.; Hou, Y.; Peng, S.; Chen, P.; Liang, X.; Zhang, J. Effects of different light intensities on the growth and biomass allocation of invasive plants *Mikania micrantha* and *Chromolaena odorata*. *J. Ecol.* **2017**, *37*, 6021–6602.
- Pan, J.H.; Huang, K.J.; Li, Z. Temporal and spatial variation of net primary productivity of vegetation in Shule River Basin from 2001 to 2010 and its relationship with climate factors. *Chin. J. Ecol.* **2017**, *37*, 12.

25. Liu, F.; Zeng, Y.G. Changes in temporal and spatial pattern of vegetation NPP in Qinghai Plateau in recent 16 years and the influence of climate and human factors. *Chin. J. Ecol.* **2019**, *39*, 1528–1540.
26. Zhou, X.; Zhu, W.; Ma, G.; Zhang, D.; Zheng, Z. Remote Sensing Assessment of Net Primary Productivity Loss of Vegetation Caused by Rare Earth Mining–Taking Ganzhou City, Jiangxi Province as an Example. *Remote Sens. Technol. Appl.* **2016**, *31*, 307–315.
27. Xiang, Y.; Li, J.; Chen, H. Research on vegetation NPP changes in Shendong mining area based on CASA model. *Hubei Agric. Sci.* **2017**, *56*, 5.
28. Zhu, W.; Pan, Y.; Hu, H.; Li, J.; Gong, P. Estimation of regional terrestrial vegetation NPP based on GIS and RS—Taking Inner Mongolia, China as an example. *J. Remote Sens.* **2005**, *009*, 300–307.
29. Chen, J.M.; Chen, X.; Ju, W. Effects of vegetation heterogeneity and surface topography on spatial scaling of net primary productivity. *Biogeosciences* **2013**, *10*, 4879–4896. [[CrossRef](#)]
30. Fujun, C.; Yanjun, S.; Qian, L.; Ying, G.; Limei, X. Research on the Spatial and Temporal Changes of NPP in China’s Terrestrial Ecosystem in Recent 30 Years. *Geoscience* **2011**, *31*, 1409–1414.
31. Yang, H.; Zhou, W.; Shi, P.Q.; Huang, L. Spatial and temporal change pattern of grassland NPP in Inner Mongolia and its coupling relationship with hydrothermal factors. *Res. Water Soil Conserv.* **2019**, *26*, 234–240.
32. Hong, L.; Shen, Y.; Ma, H.; Zhang, P.; Huo, X.; Wen, H. Temporal and spatial changes of net primary productivity of vegetation in Ningxia from 2000 to 2019 and its driving factors. *Chin. J. Appl. Ecol.* **2022**, *33*, 1–10.
33. Yi, W.; Cong, Z.; Li, Z.; Liqin, D.; Kun, Z. Temporal and spatial dynamic changes of net primary productivity of vegetation in Ruorgai Plateau from 2000 to 2019 and its relationship with climate factors. *J. Southwest For. Univ. (Nat. Sci.)* **2022**, *42*, 52–61.
34. Wang, J.; Wu, M. Spatial and temporal changes of primary productivity of vegetation in Mentougou District, Beijing, 2003–2014. *J. East China Norm. Univ.* **2018**, *2018*, 163–170.
35. Liu, F.; Chi, Y.; Wang, Z.; Wang, Y. Analysis on the potential of NPP included in the ecological statistical indicator system—Taking NPP measurement and spatial analysis in Beijing as an example. *J. Ecol. Environ.* **2009**, *18*, 960–966.
36. Cheng, F.; Liu, S.; Zhang, Y.; Yin, Y.; Hou, X. The impact of land use change on net primary productivity in Beijing based on MODIS sequence. *J. Ecol.* **2017**, *37*, 5924–5934.
37. Su, W.; Yu, X.; Lu, X.; Fan, J.; Zhang, Y. Research on the impact of climate change on NPP of North China Larch Forest in Beijing Mountain Area. *Guangdong Agric. Sci.* **2012**, *39*, 69–72.
38. Ma, B.; Jing, J.; Xu, Y.; He, H.; Liu, B. Study on the temporal and spatial changes of vegetation NPP in karst areas of Yunnan, Guizhou and Guangxi from 2000 to 2019 and its relationship with climate change. *J. Ecol. Environ.* **2021**, *30*, 2285–2293.
39. Zhou, J.; He, Z.; Zhang, Z.; Chen, L. Analysis of the relationship between the spatial and temporal pattern of vegetation NPP and meteorological factors. *Geospat. Inf.* **2018**, *16*, 25–28+31+10.
40. Xie, S.; Liu, Y.; Yao, F. Spatial and temporal change of NDVI in Beijing from 1998 to 2015 and its response to climate factors. *Res. Water Soil Conserv.* **2020**, *27*, 190–196+202+2.
41. Liu, Z.; Chen, J. Correlation between spatial and temporal changes of vegetation and climate factors in Beijing. *Geol. Bull.* **2021**, *40*, 2159–2166.
42. Mu, S.; You, Y.; Zhu, C.; Zhou, K. Temporal and spatial pattern of grassland vegetation precipitation utilization efficiency in northwest China. *J. Ecol.* **2017**, *37*, 1458–1471.
43. Guo, L.; Hao, C.; Wu, S.; Zhao, D.; Gao, J. CENTRY simulation study on the change characteristics of grassland NPP in Inner Mongolia and its sensitivity to climate change. *Geogr. Res.* **2016**, *35*, 271–284.